

Resolving Sentiment Discrepancy for Multimodal Sentiment Detection via Semantics Completion and Decomposition

Daiqing Wu, Dongbao Yang, Huawen Shen, Can Ma, Yu Zhou
 Institute of Information Engineering, Chinese Academy of Sciences
 University of Chinese Academy of Sciences
 TMCC, College of Computer Science, Nankai University
 China

ABSTRACT

With the proliferation of social media posts in recent years, the need to detect sentiments in multimodal (image-text) content has grown rapidly. Since posts are user-generated, the image and text from the same post can express different or even contradictory sentiments, leading to potential **sentiment discrepancy**. However, existing works mainly adopt a single-branch fusion structure that primarily captures the consistent sentiment between image and text. The ignorance or implicit modeling of discrepant sentiment results in compromised unimodal encoding and limited performances. In this paper, we propose a semantics Completion and Decomposition (CoDe) network to resolve the above issue. In the semantics completion module, we complement image and text representations with the semantics of the OCR text embedded in the image, helping bridge the sentiment gap. In the semantics decomposition module, we decompose image and text representations with exclusive projection and contrastive learning, thereby explicitly capturing the discrepant sentiment between modalities. Finally, we fuse image and text representations by cross-attention and combine them with the learned discrepant sentiment for final classification. Extensive experiments conducted on four multimodal sentiment datasets demonstrate the superiority of CoDe against SOTA methods.

CCS CONCEPTS

• **Information systems** → **Sentiment analysis**; *Multimedia information systems*.

KEYWORDS

multimodal sentiment detection, sentiment discrepancy, semantics completion, semantics decomposition

1 INTRODUCTION

Multimodal sentiment detection aims to detect sentiments embedded in image-text posts. With the popularity of social media and the exponential increase in posts, it demonstrates broad applications in opinion mining, psychological health, and business intelligence [47]. As a result, it attracts substantial attention from both academic and industrial communities [44, 45]. Unlike unimodal data, image-text posts contain abundant information from both visual and textual modalities. The complexity of effectively encoding and fusing modalities becomes the core focus of researchers.

Previous studies primarily focus on modeling inter-modal interactions [33, 38–41] and inter-sample relationships [19, 42]. Despite their successes, they have not properly handled **sentiment discrepancy**—that the sentiments embedded in the image and text

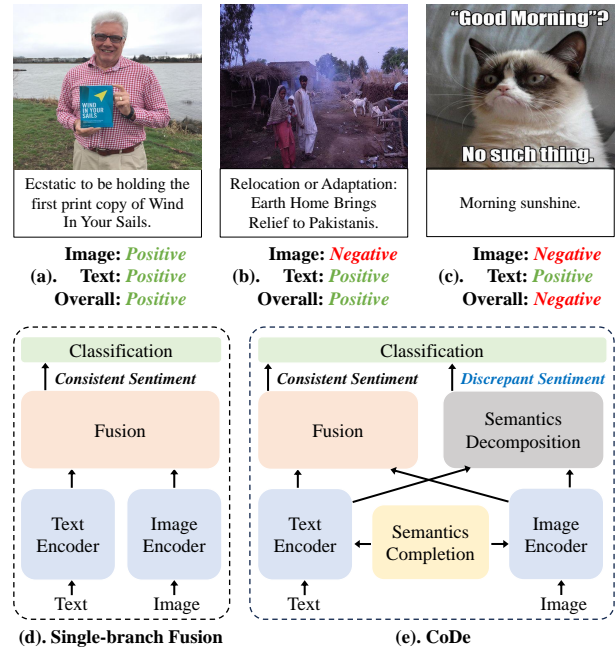


Figure 1: (a) Posts with consistent sentiments between modalities. (b,c) Posts with sentiment discrepancy. (d, e) Structures of Single-branch fusion and CoDe.

from the same post can be different or even contradictory, a prevalent issue in posts collected from social media. As illustrated in Fig. 1 (b), the image portrays a scene of ruins following a disaster, evoking a negative sentiment. In contrast, the text describes that an organization provides solutions for the refugees, shifting the overall sentiment to a positive tone. Compared to posts with consistent sentiments (like Fig. 1 (a)), those with sentiment discrepancy pose a greater challenge for previous models.

Concretely, most of them [19, 33, 35, 38, 40–42] employ a similar single-branch fusion structure, as illustrated in Fig. 1 (d). Unimodal features are extracted separately and fed into a fusion module, which mainly captures the consistent sentiment embedded in their shared semantics for classification. As a result, the discrepant sentiment is ignored or modeled implicitly. When encountering sentiment discrepancy during training—which accounts for 26.0%–73.9% (Table 2) of posts across datasets [2, 26, 41], the consistent sentiment is insufficient to represent the entire post. Consequently, both image and text representations overfit to the consistent sentiment, compromising the unimodal encoding and, in turn, the fused multimodal representation. Although MVCN [35] and some other

video-targeted studies [8, 18, 46] attempt to address the modality gap, they mainly focus on information granularity instead of sentiments. This leaves sentiment discrepancy still nascent and under-explored for sentiment detection of image-text posts.

To comprehensively resolve sentiment discrepancy, we propose a semantics Completion and Decomposition (**CoDe**) method, as depicted in Fig. 1 (e). It possesses two additional modules: **semantics completion** and **semantics decomposition**.

(1) In semantics completion module, we leverage OCR (Optical Character Recognition) texts embedded in images through attention mechanisms [25, 32] to semantically complement both image and text representations. According to statistics (Table 2), OCR text is present in the images of 63% posts. It can furnish contextual semantics for both modalities, playing a crucial role in alleviating sentiment discrepancy. As shown in Fig. 1 (c), the image depicts a grumpy cat with a negative sentiment, while the text conveys a positive attitude toward the morning. There exists apparent sentiment discrepancy between them. The OCR text: “Good Morning? No Such thing.” can function as a semantic bridge, contributing to narrowing the sentiment gap.

(2) In semantics decomposition module, we use two projectors to decompose image and text representation into semantically exclusive sub-representations, thereby explicitly capturing the discrepant sentiment. Specifically, we guide the first sub-representations to learn modality-shared sentiments through contrastive learning and supervise the second sub-representations to obtain modality-private sentiments by an exclusive constraint on projectors. We then adopt subtraction on the second sub-representations to capture the inter-modal discrepant sentiment, which is later concatenated with the consistent sentiment obtained in the fusion module for classification. Semantics decomposition avoids the over-reliance of the single-branch fusion structure on the consistent sentiment and is conducive to the comprehensive encoding of the post.

Our main contributions can be summarized as follows:

- We propose a method called **CoDe** to resolve **sentiment discrepancy**. It includes semantics completion module that complements image and text representations with OCR text semantics to alleviate sentiment discrepancy, and semantics decomposition module that decomposes image and text representations to explicitly capture the inter-modal discrepant sentiment.
- To the best of our knowledge, we are the first to utilize OCR text to handle sentiment discrepancy for multimodal sentiment detection. We focus on its shared connections with both image and text, and leverage its semantics to bridge the sentiment gap between modalities.
- We conduct extensive experiments on **four** multimodal sentiment datasets [2, 26, 41]. The results show that our model outperforms the SOTA methods, demonstrating its effectiveness.

2 RELATED WORKS

2.1 Multimodal Sentiment Detection

Multimodal sentiment detection has gradually evolved into a popular research domain with the increasing availability of multimodal data [45]. Early studies primarily focus on modeling **inter-modal interactions**. MultiSentiNet [39] and HSAN [38] concatenate visual and textual features. CoMN [40] introduces a stackable memory

hop structure, and MIMN [33] expands it to support aspect-level classification. TomBERT [43] employs the encoder of Transformer [32] to perform a cross-attention interaction. MVAN [41] proposes a multi-layer perceptron and a stacking-pooling module. Recent works consider **inter-sample relationships**. MGNNs [42] applies GNN to model the global characteristics of samples. CLMLF [19] proposes two contrastive learning tasks to learn common features related to sentiments and samples. More recently, MVCN [35] shifts focus toward **modality gap**. It tackles the challenge of modality heterogeneity—that modalities have different information granularity. Similar to MVCN, we also focus on **modality gap**, but from a different perspective. We aim to resolve sentiment discrepancy between modalities, which has not been fully addressed by methods in this field.

2.2 Modality Gap

In multimodal data, various modalities have different semantics and information granularity, constituting to the modality gap. In recent years, it has drawn widespread attention across various fields, such as vision-language pre-training [11, 17], crisis event categorization [1, 37], multimodal sarcasm detection [36] and video-targeted sentiment analysis [8, 18, 46].

For studies focusing on **inter-modal semantics differences**, in vision-language pre-training, ALBEF [17] introduces a self-distillation structure by providing pseudo-targets from a momentum model. Jiang *et al.*[11] propose a contrastive learning strategy regulated by progressively refined cross-modal similarity. In crisis event categorization, Abavisani *et al.*[1] present a cross-attention module to filter uninformative and misleading components from weak modalities. CIMHIM [37] adopts a post-fusion of unimodal classification results. In multimodal sarcasm detection, DIP [36] leverages sample distribution to model the inter-modal semantic similarity. Among these studies, DIP is most similar to ours. However, it aims to determine **whether there exists sentiment discrepancy**, while our model needs to **perceive the specific discrepant sentiment**.

For studies focusing on **information granularity**, in video-targeted sentiment analysis, MISA [8] projects modalities into modality-invariant and -specific subspaces to minimize information redundancy. Based on MISA, TAILOR [46] and DMD [18] propose an adversarial refinement module and an adaptive knowledge distillation, respectively, to strengthen the diversity of each modality. In multimodal sentiment detection, MVCN [35] also tackles a similar problem. Compared with them, we focus on **sentiment discrepancy**, which originates from **inter-modal semantics differences**. Inspired by their success, we design the semantics decomposition module based on MISA, and take one step further to guide the sentiment learning of decomposed representations. This enables our model to **explicitly capture the modality-private sentiment** rather than **other redundant modality-private information**.

2.3 OCR Text

Images frequently contain OCR texts, which are vital for human comprehension of visual contents [12, 34]. Previous studies on object detection and recognition have utilized such information, verifying its benefits in understanding images. Karaoglu *et al.*[13] use recognized text as complements to visual cues for fine-grained

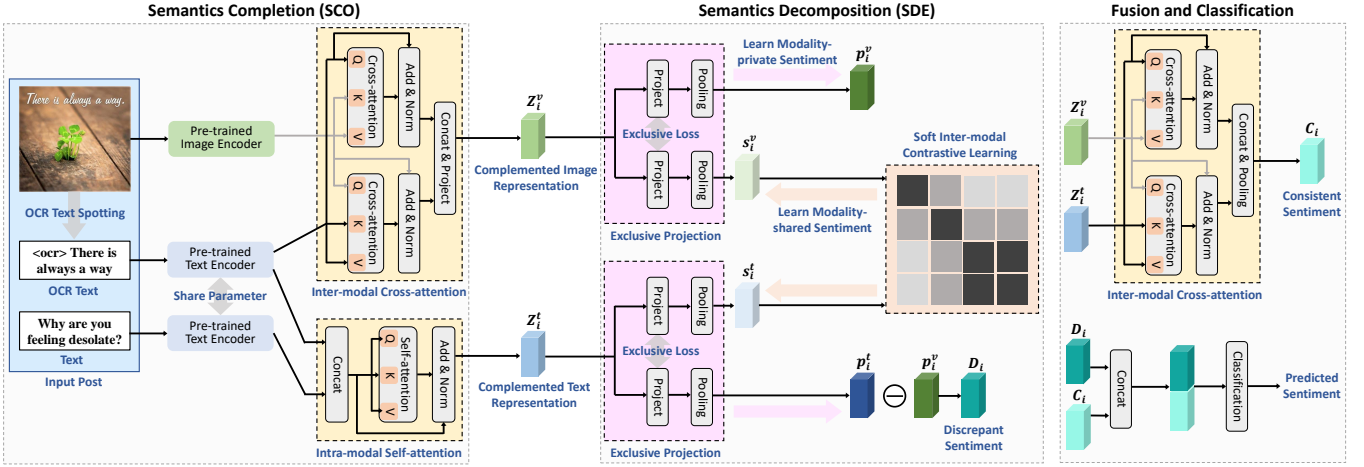


Figure 2: Pipeline of CoDe network. Given an input post, we first extract OCR text by off-the-shelf tools. We then use pre-trained encoders to process the image, OCR text, and text to obtain their representations. Subsequently, we develop two attention modules to complement image and text representations with OCR text semantics. Following this, we decompose each complemented representation into two semantically exclusive sub-representations by exclusive projection. One sub-representation learns the modality-shared sentiment through a soft inter-modal contrastive learning. The other sub-representation is forced to learn the modality-private sentiment by an exclusive loss. Finally, we subtract the sub-representations that embed modality-private sentiment to capture the discrepant sentiment between image and text, and concatenate it with the consistent sentiment obtained from global fusion for classification.

classification and logo retrieval. Con-Text [14] directly concatenates image and OCR text features. TextPlace [10] utilizes the invariance of OCR text to illumination changes for robust visual place recognition. ViSTA [4] devises a unified framework for deep interaction between modalities. Compared with serving as object accessories in natural scenes [14], OCR text in user-generated posts conveys more subjective information. Related multimodal studies [3, 27, 37] achieve improvements by incorporating OCR text into their models, yet they neglect its connections with other modalities and only utilize it as independent knowledge. In contrast, we leverage OCR information more extensively, using it as shared contextual information to handle the sentiment discrepancy between image and text.

3 METHOD

The overall architecture of our proposed CoDe network is shown in Fig. 2. It consists of three steps: Semantics Completion, Semantics Decomposition, Fusion and Classification.

3.1 Task Definition

The objective of our model is to detect the specific sentiments embedded in image-text posts. The input of model is a set of posts: $\{(v_1, t_1), (v_2, t_2), \dots, (v_N, t_N)\}$, where v_i, t_i represent the image and text of i th post, respectively. The model needs to classify each of the post (v_i, t_i) into a single sentiment category c_i that belongs to a pre-defined category set.

3.2 Semantics Completion

Given a post (v_i, t_i) , we first process image v_i by two off-the-shelf models, DBNet [21] and SAR [16], to extract OCR text o_i . DBNet

detects the potential regions containing OCR text, and SAR recognizes the contents within these regions. o_i is a sequence of words, similar to text t_i .

We then encode image v_i by pre-trained image encoder SwinT [22], text t_i by pre-trained text encoder BERT [5], to obtain image representation $z_i^v \in \mathbb{R}^{I \times F}$ and text representation $z_i^t \in \mathbb{R}^{L \times F}$. I is the number of image patches, L is the max text length, and F is the feature dimension. For OCR text o_i , as it also belongs to textual modality, we encode it by a shared-parameter BERT to obtain its representation $z_i^o \in \mathbb{R}^{L \times F}$. To distinguish two kinds of textual inputs, we add an $\langle \text{ocr} \rangle$ token at the beginning of OCR text o_i . In cases where OCR text is absent from the image, this token also serves as a placeholder to maintain the continuity of the computations.

Subsequently, we incorporate the contextual semantics of OCR text into both image and text representations through two kinds of attention modules [25, 32]. A general attention head is formulated as:

$$A(q, k, v) = \text{softmax}\left(\frac{QK^T}{\sqrt{d}}\right)V. \quad (1)$$

$$Q = qP_Q, K = kP_K, V = vP_V. \quad (2)$$

Vectors query(q), key(k), value(v) are first linear projected to a common subspace by matrices P_Q, P_K, P_V . Then, the correlation between Q and K is calculated via dot product similarity divided by the square root of feature dimension d (equals to F in our cases) and a softmax normalization. Finally, V is multiplied by this correlative matrix for information fusion. For image representation, we develop an inter-modal cross-attention:

$$Z_i^v = P_{ca}[A(z_i^o, z_i^v, z_i^v) + z_i^o, A(z_i^v, z_i^o, z_i^o) + z_i^v] \in \mathbb{R}^{I \times F}. \quad (3)$$

Table 1: Mapping M from sentiment categories (left columns) to discrete numerical values (right columns) of datasets [2, 26, 41]. MVSA-* refers to MVSA-Single and MVSA-Multiple. The categories of HFM represent whether the post expresses sarcasm rather than the post sentiment. Due to the similarity of the task targets, it is recently adopted as a benchmark dataset for testing the generalization ability of models.

MVSA-*		TumEmo			HFM		
Positive	0	Love	0	Sad	4	Positive	0
Neutral	1	Happy	1	Angry	5	Negative	1
Negative	2	Calm	2	Fear	6		
		Bored	3				

P_{ca} is a learnable $\mathbb{R}^{I \times (I+L)}$ matrix and $[\cdot]$ is concatenate operation. We calculate and concatenate an OCR-text-guided image attention and an image-guided OCR text attention, which is then fed into linear projector P_{ca} to obtain the complemented image representation Z_i^v . For text representation, we develop an intra-modal self-attention:

$$Z_i^t = A([z_i^t, z_i^o], [z_i^t, z_i^o], [z_i^t, z_i^o]) + [z_i^t, z_i^o] \in \mathbb{R}^{2L \times F}. \quad (4)$$

We directly concatenate z_i^t and z_i^o and apply self-attention to it to obtain the complemented text representation Z_i^t .

The asymmetry in formulations between Z_i^v and Z_i^t arises from the differences between modalities. Both text t_i and OCR text o_i belong to textual modality and are encoded by BERT with shared parameters. In this encoding, each channel of z_i^t and z_i^o represents the semantics of a textual word [5], allowing for direct concatenation to maintain feature consistency across dimensions. However, in the case of image representation z_i^v , where each channel represents the semantics of a visual patch [6], such consistency no longer holds. Directly concatenating them would introduce additional alignment burdens during early training stages, which is not conducive to the model’s learning process.

In summary, this module extracts OCR text and uses it to semantically complement both image and text representations. It connects the image and text with the shared OCR text semantics, helping to alleviate sentiment discrepancy between them.

3.3 Semantics Decomposition

In this module, we explicitly capture the discrepant sentiment to avoid the model’s over-reliance on the consistent sentiment, enabling the model to learn more comprehensive multi-modal representations.

We first devise an exclusive projection to decouple sentiments embedded in the complemented representations Z_i^v and Z_i^t :

$$s_i^v = Pool(Z_i^v P_s^v), \quad p_i^v = Pool(Z_i^v P_p^v) \in \mathbb{R}^F. \quad (5)$$

$$s_i^t = Pool(Z_i^t P_s^t), \quad p_i^t = Pool(Z_i^t P_p^t) \in \mathbb{R}^F. \quad (6)$$

We feed them into four projectors, with each followed by an average pooling layer, to obtain modality-shared sub-representations s_i^v, s_i^t and modality-private sub-representations p_i^v, p_i^t . Projectors $P_s^v, P_p^v, P_s^t, P_p^t$ are learnable $\mathbb{R}^{F \times F}$ matrices with row-wise normalization.

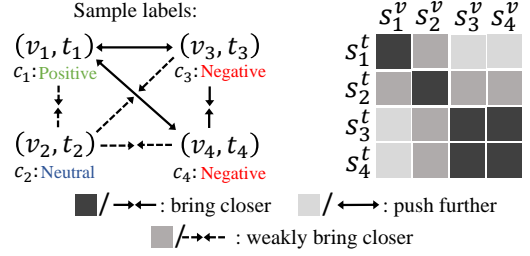


Figure 3: An example of the soft inter-modal contrastive learning. Each s_i^v is brought closer to its counterpart s_i^t . (s_1^v, s_3^t), with $w_{1,3} = 0$, is treated as a negative pair and pushed away. (s_1^v, s_2^t), with $w_{1,2} = 0.5$, are treated as a partial positive pair and weakly brought closer. (s_3^v, s_4^t), with $w_{3,4} = 1$, is treated as a positive pair and brought closer.

They are constrained by an exclusive loss with a hyperparameter σ controlling the distinction between them:

$$\begin{aligned} \mathcal{L}_{exc} = & \max(\sigma - \|P_s^v - P_p^v\|_F, 0) \\ & + \max(\sigma - \|P_s^t - P_p^t\|_F, 0). \end{aligned} \quad (7)$$

Inspired by the multi-class N-pair loss [30, 31], we guide s_i^v, s_i^t in learning the modality-shared sentiment through a soft inter-modal contrastive learning. We construct each sample pair with a modality-shared image sub-representation and a modality-shared text sub-representation, and treat pairs with the same sentiment categories as positive pairs. Different from regular contrastive learning that treats all other pairs as negative pairs, we consider sample pairs with closely related but non-identical sentiment categories as partial positive pairs. The contrastive loss is thereby formulated as:

$$\mathcal{L}_{con} = -\log \frac{\sum_j w_{i,j} \exp(s_i^v \cdot s_j^t / \tau)}{\sum_j \exp(s_i^v \cdot s_j^t / \tau)}. \quad (8)$$

τ is the temperature hyperparameter. Weight $w_{i,j}$ reflects the correlation between the sentiment categories c_i and c_j of the i th and j th posts. In order to acquire such correlations, we construct a mapping M (as shown in Table 1) that converts sentiment categories to discrete numerical values by referring to Ekman’s emotion model [7]. Following this, we define the weight $w_{i,j}$ as the normalized distance between $M(c_i)$ and $M(c_j)$:

$$w_{i,j} = \frac{|M(c_i) - M(c_j)|}{|\max(M(*)) - \min(M(*))|} \in [0, 1]. \quad (9)$$

An example is illustrated in Fig. 3 for an intuitive understanding of the soft inter-modal contrastive learning.

Consequently, s_i^v, s_i^t learn the modality-shared sentiment. Obtained by the exclusive projection, p_i^v, p_i^t learn the modality-private sentiment that distinct from s_i^v, s_i^t . As a partial objective of the inter-modal contrastive learning, the feature spaces of image and text sub-representations are aligned [29]. Therefore, we can capture the discrepant sentiment through subtracting p_i^t by p_i^v :

$$D_i = p_i^t - p_i^v \in \mathbb{R}^F. \quad (10)$$

Table 2: Statistics of datasets. Column 2 represents the total number of posts. Columns 3-5 represent the number of posts of each split. Column 6 represents the number of posts containing OCR texts. We consider OCR texts to be present if they are detectable by DBNet [21]. Column 7 represents the number of posts containing sentiment discrepancy (SD). We consider a post contains sentiment discrepancy if the sentiment categories of its image and text are different. Unimodal sentiment categories are provided by MVSA-Single and MVSA-Multiple. As for TumEmo and HFM, we adopt pre-trained BERTweet [28] and ViT [6] as grounding sentiment evaluators to obtain this information. Column 8 represents the number of posts containing both OCR texts and sentiment discrepancy.

Dataset	Total	Train	Val	Test	OCR (%)	SD (%)	OCR&SD (%)
MVSA-Single [26]	4511	3608	451	452	2747 (60.9%)	1919 (42.5%)	1249 (27.7%)
MVSA-Multiple [26]	17024	13618	1703	1703	11286 (66.3%)	4425 (26.0%)	3320 (19.5%)
TumEmo [41]	195265	156217	19524	19524	120491 (61.7%)	128907 (66.0%)	80679 (41.3%)
HFM [2]	24635	19816	2410	2409	18511 (75.1%)	18208 (73.9%)	13388 (54.3%)

3.4 Fusion and Classification

Following previous works [19, 42], we conduct a global fusion of Z_i^v and Z_i^t to capture the consistent sentiment between modalities. We employ the inter-modal cross-attention module similar to Eq. (3):

$$C_i = Pool([A(Z_i^v, Z_i^t, Z_i^t) + Z_i^v, A(Z_i^t, Z_i^v, Z_i^v) + Z_i^t]) \in \mathbb{R}^F. \quad (11)$$

$Pool(\cdot)$ represents an average pooling layer.

Finally, we concatenate the consistent sentiment C_i and the discrepant sentiment D_i , and feed the result into a projector P_{cls} for classification:

$$\mathcal{L}_{cls} = Cross - entropy([C_i, D_i]P_{cls}). \quad (12)$$

The total loss is the combination of \mathcal{L}_{cls} , \mathcal{L}_{exc} and \mathcal{L}_{con} :

$$\mathcal{L}_{total} = \mathcal{L}_{cls} + \mathcal{L}_{exc} + \mathcal{L}_{con}. \quad (13)$$

4 EXPERIMENT

4.1 Datasets

We conduct experiments on four publicly available multimodal sentiment datasets: MVSA-Single, MVSA-Multiple [26], TumEmo [41], and HFM [2]. The detailed statistics are presented in Table 2. **MVSA-Single** and **MVSA-Multiple** are both collected from Twitter¹. Each of their posts is annotated with an image sentiment category and a text sentiment category. We assign multimodal categories to posts following Xu *et al.* [39]. **TumEmo** is a large-scale weak-supervision dataset collected from Tumblr², with an overall sentiment category assigned to each sample. **HFM** is a popular multimodal sarcasm detection dataset. The categories of HFM represent whether the post expresses sarcasm rather than the post sentiment. It has been adopted since CLMLF [19] to test the generalization ability of models. For a fair comparison, we follow the pre-processing approaches and adopt the evaluation metrics in [41] and [2]. Specifically, we report accuracy (**acc**) and weighted-F1 (**w-F1**) for MVSA-Single, MVSA-Multiple and TumEmo; accuracy (**acc**) and macro-F1 (**m-F1**) for HFM.

¹<https://twitter.com>

²<http://tumblr.com>

4.2 Implementation Details

All our implementations are based on PyTorch. We adopt the same settings across all four datasets. Our model is trained for 20 epochs with a batch size of 16. The initial learning rate is set to 5e-5 for the image encoder, 2e-5 for the text encoder, 1e-3 for the classification layer, and 2e-4 for other parameters. We adopt AdamW optimizer [24] and decay the learning rate using a cosine scheduler [23]. The threshold σ in Eq. (7) is set to 0.1, the temperature τ in Eq. (8) is set to 0.07.

4.3 Baselines

For unimodal comparison, we choose **CNN** [15], **Bi-LSTM** [48], **BERT** [5] as text baselines, and **ResNet** [9], **ViT** [6], **SwinT** [22] as image baselines. These models are commonly adopted for classification tasks in their corresponding modalities.

For multimodal comparison, as introduced in Section 2.1, we choose **MultiSentiNet** [39], **HSAN** [38], **CoMN** [40], **MVAN** [41], **MGNNS** [42], **CLMLF** [19] and **MVCN** [35] as baselines. We notice a disagreement among these works on selecting unimodal encoders, which may introduce unfair comparisons. Therefore, we additionally reproduce two latest SOTA methods: **CLMLF** and **MVCN**, together with two classic fusion strategies: concatenation (**Concat**) and cross-attention (**Att**) based on the same SwinT and BERT encoders adopted by our model.

4.4 Comparison with SOTA methods

We present the results of CoDe and SOTA methods in Table 3. Based on the results, we make the following observations: **1)** CoDe significantly outperforms unimodal methods, affirming the benefits of richer semantics in multimodal data for the comprehensive understanding of posts. **2)** Compared with multimodal methods, CoDe achieves consistent performance gain across all metrics on four datasets. These results demonstrate the necessity of resolving sentiment discrepancy in detecting sentiments in posts. **3)** CoDe achieves obvious performance gains on TumEmo and HFM, while relatively modest performance gains on MVSA-Single and MVSA-Multiple. We attribute this to the category assignment strategy [39] of MVSA-Single and MVSA-Multiple. It discards the posts with contradictory unimodal sentiment categories, thus significantly reducing the proportion of posts containing sentiment discrepancy, as presented in Table 2. For TumEmo, which is unfiltered and more

Table 3: Comparison with SOTA unimodal and multimodal methods. In addition to the results reported in previous works, we report the results of four multimodal methods under the same unimodal encoders as ours for a fair comparison. ‡ indicates the reproductive operation. **Bold** indicates the best result. Underline indicates the second best result.

Modality	Method	MVSA-Sinlge		MVSA-Multiple		TumEmo		HFM	
		Acc	W-F1	Acc	W-F1	Acc	W-F1	Acc	M-F1
Image	ResNet-50 [9]	64.67	61.55	61.88	60.98	48.10	47.75	72.77	71.38
	ViT [6]	63.78	62.26	61.94	61.19	46.35	45.94	73.09	71.52
	SwinT [‡] [22]	64.89	63.94	62.44	61.09	49.60	48.27	72.82	72.53
Text	CNN [15]	68.19	55.90	65.64	57.66	61.54	47.74	80.03	75.32
	BiLSTM [48]	70.12	65.06	67.90	67.90	61.88	51.26	81.90	77.53
	BERT [5]	71.11	69.70	67.59	66.24	62.12	60.78	83.89	83.26
Image+Text (Original Encoders)	MultiSentiNet [39]	69.84	69.84	68.86	68.11	-	-	-	-
	HSAN [38]	69.88	66.90	67.96	67.76	63.09	53.98	-	-
	CoMN [40]	70.51	70.01	69.92	69.83	64.26	59.09	-	-
	MVAN [41]	72.98	71.39	71.83	<u>70.38</u>	65.53	65.43	-	-
	MGNNS [42]	73.77	72.70	<u>72.49</u>	69.34	66.72	66.69	-	-
	CLMLF [19]	75.33	73.46	72.00	69.83	-	-	85.43	84.87
	MVCN [35]	<u>76.06</u>	74.55	72.07	70.01	-	-	85.68	85.23
Image+Text (SwinT+BERT)	Concat [‡]	73.17	72.41	69.33	68.52	70.81	69.97	84.69	84.08
	Att [‡]	74.50	73.86	70.04	67.80	71.24	71.23	85.06	84.99
	CLMLF [‡] [19]	75.61	74.79	72.17	69.74	71.30	71.27	86.64	86.40
	MVCN [‡] [35]	75.83	<u>75.33</u>	71.80	69.46	<u>71.72</u>	<u>71.58</u>	<u>87.01</u>	<u>86.50</u>
	CoDe (Ours)	76.94	76.34	72.75	70.69	73.26	73.20	88.67	88.30

Table 4: Ablation experimental results of CoDe on MVSA-Single and TumEmo. SCO abbreviates the semantics completion module. SDE abbreviates the semantics decomposition module. CL abbreviates contrastive learning.

Model	MVSA-Sinlge		TumEmo	
	Acc	W-F1	Acc	W-F1
Image-only	64.89	63.94	49.60	48.27
Text-only	71.11	69.70	62.12	60.78
w/o SCO+SDE	74.50	73.86	71.24	71.23
w/o SCO	75.39	74.25	72.53	72.45
w/o Soft Inter-modal CL	76.05	75.55	72.16	72.13
w/o SDE	76.27	75.89	72.04	71.85
CoDe	76.94	76.34	73.26	73.20

representative of the real-world distribution of posts, and HFM, which contains a frequent occurrence of sarcastic expressions, the advantages of resolving sentiment discrepancy are much more highlighted.

4.5 Ablation Experiments

To probe the effectiveness of each module, we conduct ablation experiments in Table 4. It can be observed that: 1). Both the semantics completion module and the semantics decomposition module bring significant performance gains to the model. This suggests

that complementing image and text representations with the semantics of OCR text indeed alleviates the sentiment discrepancy, and explicitly capturing the discrepant sentiment leads to more comprehensive multimodal representations. 2). The removal of the soft inter-modal contrastive learning severely impacts the effectiveness of the semantics decomposition module, underscoring the necessity of the sentiment guiding and feature alignment provided by the contrastive learning. 3). The semantics completion module improves the model stably on two datasets, while the semantics decomposition module is more efficient on TumEmo than on MVSA-Single. We conjecture that the contextual semantics of OCR text benefit the model even in case of unremarkable sentiment discrepancy, and the semantics decomposition module is more suitable for explicit sentiment discrepancy. This further explains the difference in performance improvements of CoDe on these datasets. 4). CoDe with both modules achieves the best performance, showing the modules are complementary to each other.

5 ANALYSIS

5.1 Effectiveness of OCR texts

As pointed out in Section 4.5, the performance gains brought by the semantics completion module may not be strictly confined to sentiment discrepancy. Since this module introduces additional knowledge of OCR text compared to previous works, we further investigate the source of its effectiveness. Specifically, we also incorporate OCR text into the SOTA methods by fusing it into one of

Table 5: Results of incorporating OCR text into SOTA unimodal and multimodal methods.

Modality	Method	MVSA-Sinlge		TumEmo	
		Acc	W-F1	Acc	W-F1
Image	SwinT+OCR	67.85	66.92	53.75	53.54
Text	BERT+OCR	73.39	72.65	66.17	65.89
Image+Text (SwinT+BERT)	Concat+OCR	73.67	72.99	71.21	71.20
	Att+OCR	74.94	74.25	71.46	71.43
	CLMLF+OCR	75.61	74.93	71.72	71.51
	MVCN+OCR	76.05	75.53	71.98	71.90
	CoDe (Ours)	76.94	76.34	73.26	73.20

their modalities, and present the results in Table 5. Compared with Table 3, the knowledge of OCR text only brings limited performance gains to multimodal methods, indicating that it overlaps with the knowledge of image or text in most posts, and therefore is not the main reason for our improvements. On the other hand, it brings significant performance gains in unimodal methods, demonstrating its effectiveness in complementing unimodal semantics. Based on these results, we speculate that the effectiveness of the semantics completion module arises from its tightening of the semantics connection between image and text by incorporating the shared OCR knowledge into them simultaneously. In addition to alleviating potential sentiment discrepancy, it also facilitates subsequent inter-modal interactions, including both the semantics decomposition module and the global fusion of modalities.

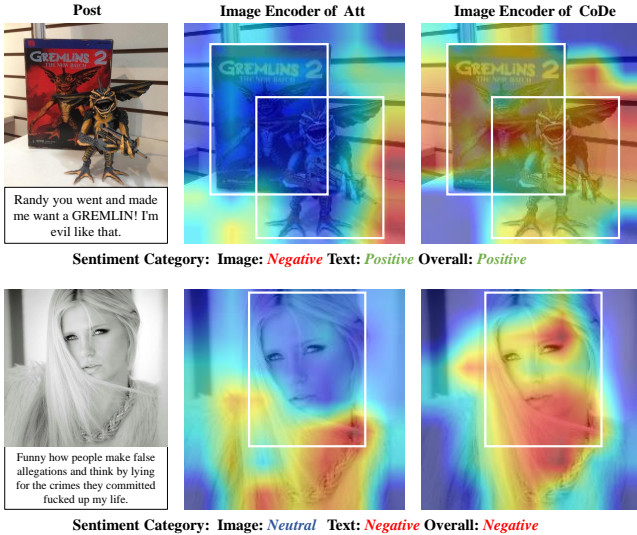


Figure 4: Attention heatmaps of the image encoders of Att and CoDe for posts containing sentiment discrepancy. The white bounding boxes circle the foreground objects through which humans intuitively perceive visual sentiments.

5.2 Attention Visualization

To visually demonstrate the advantages of CoDe in resolving sentiment discrepancy compared with the single-branch fusion structure (Fig. 1 (d)), we present the attention heatmaps of their image encoders in Fig. 4. For the single-branch fusion structure, we adopt Att, which is equivalent to CoDe with the semantics completion module and semantics decomposition module removed. We show two posts containing sentiment discrepancy, with their image sentiments distinct from the overall sentiments. It can be observed that the image encoder of Att overfits toward the overall sentiments of the posts. Instead of focusing on foreground objects that reflect the true sentiments of the images, such as the monster book and toy in the first post, the image encoder of Att mainly perceives sentiments from the backgrounds that are more aligned with the overall sentiments. This tendency leads Att to ignore certain unimodal sentiments, thereby hampering its modeling of multimodal sentiments during inference. In contrast, the image encoder of CoDe correctly concentrates on the foreground objects, sharing a similar perception with humans. It explains the effectiveness of CoDe from the perspective of unimodal encoding.

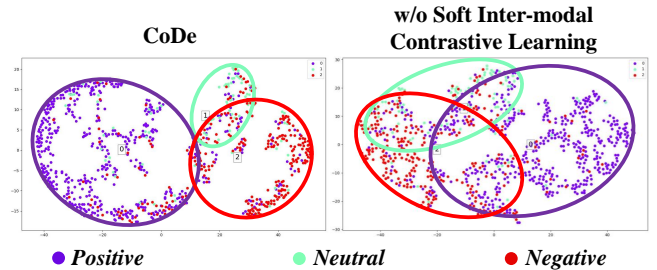


Figure 5: Distribution visualization of multimodal sentiment representations on the test set of MVSA-Single with (left) / without (right) the soft inter-modal contrastive learning.

5.3 Distribution Visualization

In Section 4.5, we verify the importance of the soft inter-modal contrastive learning for the semantics decomposition module. Interestingly, we notice that the removal of the contrastive learning results in model performance that is lower on MVSA-single than removing the entire semantics decomposition module. To further explore the influences of the contrastive learning on other modules, we apply t-SNE³ algorithm to visualize the feature distribution of the multimodal sentiment representation (the concatenation of C_i, D_i) on MVSA-Single. As demonstrated in Fig. 5, the soft inter-modal contrastive learning reduces the overlap between different sentiment categories and enables more compact data aggregation. It suggests that the contrastive learning is also beneficial to the consistent sentiment captured by modality fusion, as it is a component of the multimodal sentiment representation. We attribute this to the feature alignment of sub-representations encouraged by the contrastive learning. Such alignment extends to the complemented representations to a certain degree, thereby enabling the inter-modal cross-attention to learn more representative consistent sentiments during fusion.

³<https://github.com/mxl1990/tsne-pytorch>



Figure 6: Case study of CoDe and MVCN. Posts are arranged according to whether they contain sentiment discrepancy and OCR texts. Below each post, we present the true sentiment categories of the image, the text, and the overall post in the first row; the classification results of MVCN and CoDe in the second row.

5.4 Case Study

To concretely demonstrate the effectiveness of our model, such as which kinds of posts it has improved on, and what drawbacks it still remains, we conduct a detailed case study in Fig. 6. We adopt MVCN [35] for comparison, which is the latest SOTA method. Observably: 1). Both CoDe and MVCN can correctly predict the overall sentiments for posts without sentiment discrepancy and OCR texts. 2). When posts contain only OCR texts, MVCN fails in the second post, since it is misled by the words (e.g., sweet, birthday) in the text. CoDe, on the other hand, succeeds in both posts by tightening the semantics between image and text with OCR text. 3). For posts with sentiment discrepancy, MVCN can hardly capture the correct sentiments of posts due to its ignorance of this issue. In contrast, CoDe accurately perceives these sentiments. 4). When encountering both sentiment discrepancy and OCR texts, CoDe can still make reliable predictions by combining the semantics of OCR text to the image and text and explicitly modeling the discrepant sentiment. For example, in the first case, CoDe leverages OCR texts (e.g., Stephen Harper) as contextual semantics to understand why there exists sentiment discrepancy and what sentiment the post expresses.

Two misclassified posts are displayed on the far right of Fig. 6. In the first post, the image is an artwork with a unique style that the model is unfamiliar with. This leads to the model mistakenly categorizing it as negative based on the color tone. In the second

post, the image depicts the dismal situation of a scientist in an animation, which the model does not correctly capture. We attribute these failures to our model’s lack of robust understanding of images of different styles and the necessary external knowledge. Therefore, tackling these problems may promote further improvements in multimodal sentiment detection in the future.

6 CONCLUSION

In this paper, we propose a CoDe network to resolve sentiment discrepancy in multimodal sentiment detection. It contains two modules. In the semantics completion module, we leverage the semantics of OCR text to complement both the image and text, tightening their semantics and alleviating the sentiment gap. In the semantics decomposition module, we semantically decompose unimodal representations to explicitly capture the disparate sentiment, thereby obtaining comprehensive multimodal sentiment representation for classification. Extensive experiments on four multimodal sentiment datasets validate its effectiveness in handling sentiment discrepancy. According to a recent survey [20], large vision-language models (such as GPT-4V) still can not surpass the capabilities of expert models on some related multimodal emotion benchmarks, especially those requiring specialized domain knowledge. It highlights the necessity of further exploration of expert models.

ACKNOWLEDGMENTS

This work is supported by the National Natural Science Foundation of China (Grant NO 62376266), and by the Key Research Program of Frontier Sciences, CAS (Grant NO ZDBS-LY-7024).

REFERENCES

- [1] Mahdi Abavisani, Liwei Wu, Shengli Hu, Joel R. Tetreault, and Alejandro Jaimes. 2020. Multimodal Categorization of Crisis Events in Social Media. In *IEEE/CVF Conference on Computer Vision and Pattern Recognition, CVPR 2020, Seattle, WA, USA, June 13-19, 2020*. Computer Vision Foundation / IEEE, 14667–14677. <https://doi.org/10.1109/CVPR42600.2020.01469>
- [2] Yitao Cai, Huiyu Cai, and Xiaojun Wan. 2019. Multi-Modal Sarcasm Detection in Twitter with Hierarchical Fusion Model. In *Proceedings of the 57th Conference of the Association for Computational Linguistics, ACL 2019, Florence, Italy, July 28-August 2, 2019, Volume 1: Long Papers*. Association for Computational Linguistics, 2506–2515. <https://doi.org/10.18653/V1/P19-1239>
- [3] Junyu Chen, Jie An, Hanjia Lyu, and Jiebo Luo. 2022. Improving Visual-Textual Sentiment Analysis by Fusing Expert Features. *CoRR* abs/2211.12981 (2022). <https://doi.org/10.48550/ARXIV.2211.12981> arXiv:2211.12981
- [4] Mengjun Cheng, Yipeng Sun, Longchao Wang, Xiongwei Zhu, Kun Yao, Jie Chen, Guoli Song, Junyu Han, Jingtuo Liu, Errui Ding, and Jingdong Wang. 2022. ViSTA: Vision and Scene Text Aggregation for Cross-Modal Retrieval. In *IEEE/CVF Conference on Computer Vision and Pattern Recognition, CVPR 2022, New Orleans, LA, USA, June 18-24, 2022*. Computer Vision Foundation / IEEE, 5174–5183. <https://doi.org/10.1109/CVPR52688.2022.00512>
- [5] Jacob Devlin, Ming-Wei Chang, Kenton Lee, and Kristina Toutanova. 2019. BERT: Pre-training of Deep Bidirectional Transformers for Language Understanding. In *Proceedings of the 2019 Conference of the North American Chapter of the Association for Computational Linguistics: Human Language Technologies, NAACL-HLT 2019, Minneapolis, MN, USA, June 2-7, 2019, Volume 1 (Long and Short Papers)*. Association for Computational Linguistics, 4171–4186. <https://doi.org/10.18653/V1/N19-1423>
- [6] Alexey Dosovitskiy, Lucas Beyer, Alexander Kolesnikov, Dirk Weissenborn, Xiuhua Zhai, Thomas Unterthiner, Mostafa Dehghani, Matthias Minderer, Georg Heigold, Sylvain Gelly, Jakob Uszkoreit, and Neil Houlsby. 2021. An Image is Worth 16x16 Words: Transformers for Image Recognition at Scale. In *9th International Conference on Learning Representations, ICLR 2021, Virtual Event, Austria, May 3-7, 2021*. OpenReview.net. <https://openreview.net/forum?id=YicbFdNTTy>
- [7] Paul Ekman. 1992. An argument for basic emotions. *Cognition & emotion* 6, 3-4 (1992), 169–200.
- [8] Devamanyu Hazarika, Roger Zimmermann, and Soujanya Poria. 2020. MISA: Modality-Invariant and -Specific Representations for Multimodal Sentiment Analysis. In *The 28th ACM International Conference on Multimedia, Virtual Event / Seattle, WA, USA, October 12-16, 2020*. ACM, 1122–1131. <https://doi.org/10.1145/3394171.3413678>
- [9] Kaiming He, Xiangyu Zhang, Shaoqing Ren, and Jian Sun. 2016. Deep Residual Learning for Image Recognition. In *IEEE/CVF Conference on Computer Vision and Pattern Recognition, CVPR 2016, Las Vegas, NV, USA, June 27-30, 2016*. Computer Vision Foundation / IEEE, 770–778. <https://doi.org/10.1109/CVPR.2016.90>
- [10] Ziyang Hong, Yvan R. Petillot, David Lane, Yishu Miao, and Sen Wang. 2019. TextPlace: Visual Place Recognition and Topological Localization Through Reading Scene Texts. In *IEEE/CVF International Conference on Computer Vision, ICCV 2019, Seoul, Korea (South), October 27 - November 2, 2019*. Computer Vision Foundation / IEEE, 2861–2870. <https://doi.org/10.1109/ICCV.2019.00295>
- [11] Chaoya Jiang, Wei Ye, Haiyang Xu, Songfang Huang, Fei Huang, and Shikun Zhang. 2023. Vision Language Pre-training by Contrastive Learning with Cross-Modal Similarity Regulation. In *Proceedings of the 61st Annual Meeting of the Association for Computational Linguistics (Volume 1: Long Papers), ACL 2023, Toronto, Canada, July 9-14, 2023*. Association for Computational Linguistics, 14660–14679. <https://doi.org/10.18653/V1/2023.ACL-LONG.819>
- [12] Tilke Judd, Krista A. Ehinger, Frédo Durand, and Antonio Torralba. 2009. Learning to Predict Where Humans Look. In *IEEE/CVF International Conference on Computer Vision, ICCV 2009, Kyoto, Japan, September 27 - October 4, 2009*. Computer Vision Foundation / IEEE, 2106–2113. <https://doi.org/10.1109/ICCV.2009.5459462>
- [13] Sezer Karaoglu, Ran Tao, Theo Gevers, and Arnold W. M. Smeulders. 2017. Words Matter: Scene Text for Image Classification and Retrieval. *IEEE Transactions on Multimedia* 19, 5 (2017), 1063–1076. <https://doi.org/10.1109/TMM.2016.2638622>
- [14] Sezer Karaoglu, Ran Tao, Jan C. van Gemert, and Theo Gevers. 2017. Con-Text: Text Detection for Fine-Grained Object Classification. *IEEE Transactions on Image Processing* 26, 8 (2017), 3965–3980. <https://doi.org/10.1109/TIP.2017.2707805>
- [15] Yoon Kim. 2014. Convolutional Neural Networks for Sentence Classification. In *Proceedings of the 2014 Conference on Empirical Methods in Natural Language Processing, EMNLP 2014, October 25-29, 2014, Doha, Qatar, A meeting of SIGDAT, a Special Interest Group of the ACL*. ACL, 1746–1751. <https://doi.org/10.3115/V1/D14-1181>
- [16] Hui Li, Peng Wang, Chunhua Shen, and Guyu Zhang. 2019. Show, Attend and Read: A Simple and Strong Baseline for Irregular Text Recognition. In *The Thirty-Third AAAI Conference on Artificial Intelligence, AAAI 2019, The Thirty-First Innovative Applications of Artificial Intelligence Conference, IAAI 2019, The Ninth AAAI Symposium on Educational Advances in Artificial Intelligence, EAAI 2019, Honolulu, Hawaii, USA, January 27 - February 1, 2019*. AAAI Press, 8610–8617. <https://doi.org/10.1609/AAAI.V33I01.33018610>
- [17] Junnan Li, Ramprasaath R. Selvaraju, Akhilesh Gotmare, Shafiq R. Joty, Caiming Xiong, and Steven Chu-Hong Hoi. 2021. Align Before Fuse: Vision and Language Representation Learning with Momentum Distillation. In *Advances in Neural Information Processing Systems 34: Annual Conference on Neural Information Processing Systems 2021, NeurIPS 2021, December 6-14, 2021, virtual*. 9694–9705. <https://proceedings.neurips.cc/paper/2021/hash/505259756244493872b7709a8a01b536-Abstract.html>
- [18] Yong Li, Yuanzhi Wang, and Zhen Cui. 2023. Decoupled Multimodal Distilling for Emotion Recognition. In *IEEE/CVF Conference on Computer Vision and Pattern Recognition, CVPR 2023, Vancouver, BC, Canada, June 17-24, 2023*. Computer Vision Foundation / IEEE, 6631–6640. <https://doi.org/10.1109/CVPR52729.2023.00641>
- [19] Zhen Li, Bing Xu, Conghui Zhu, and Tiejun Zhao. 2022. CLMLF: A Contrastive Learning and Multi-Layer Fusion Method for Multimodal Sentiment Detection. In *Findings of the Association for Computational Linguistics: NAACL 2022, Seattle, WA, United States, July 10-15, 2022*. Association for Computational Linguistics, 2282–2294. <https://doi.org/10.18653/V1/2022.FINDINGS-NAACL.175>
- [20] Zheng Lian, Licai Sun, Haiyang Sun, Kang Chen, Zhuofan Wen, Hao Gu, Shun Chen, Bin Liu, and Jianhua Tao. 2023. GPT-4V with Emotion: A Zero-shot Benchmark for Multimodal Emotion Understanding. *CoRR* abs/2312.04293 (2023). <https://doi.org/10.48550/ARXIV.2312.04293> arXiv:2312.04293
- [21] Minghui Liao, Zhaoyi Wan, Cong Yao, Kai Chen, and Xiang Bai. 2020. Real-Time Scene Text Detection with Differentiable Binarization. In *The Thirty-Fourth AAAI Conference on Artificial Intelligence, AAAI 2020, The Thirty-Second Innovative Applications of Artificial Intelligence Conference, IAAI 2020, The Tenth AAAI Symposium on Educational Advances in Artificial Intelligence, EAAI 2020, New York, NY, USA, February 7-12, 2020*. AAAI Press, 11474–11481. <https://doi.org/10.1609/AAAI.V34I07.6812>
- [22] Ze Liu, Yutong Lin, Yue Cao, Han Hu, Yixuan Wei, Zheng Zhang, Stephen Lin, and Baining Guo. 2021. Swin Transformer: Hierarchical Vision Transformer Using Shifted Windows. In *IEEE/CVF International Conference on Computer Vision, ICCV 2021, Montreal, QC, Canada, October 10-17, 2021*. IEEE, 9992–10002. <https://doi.org/10.1109/ICCV48922.2021.00986>
- [23] Ilya Loshchilov and Frank Hutter. 2017. SGDR: Stochastic Gradient Descent with Warm Restarts. In *5th International Conference on Learning Representations, ICLR 2017, Toulon, France, April 24-26, 2017, Conference Track Proceedings*. OpenReview.net. <https://openreview.net/forum?id=Skq89Scxx>
- [24] Ilya Loshchilov and Frank Hutter. 2019. Decoupled Weight Decay Regularization. In *7th International Conference on Learning Representations, ICLR 2019, New Orleans, LA, USA, May 6-9, 2019*. OpenReview.net. <https://openreview.net/forum?id=Bkg6RiCqY7>
- [25] Thang Luong, Hieu Pham, and Christopher D. Manning. 2015. Effective Approaches to Attention-Based Neural Machine Translation. In *Proceedings of the 2015 Conference on Empirical Methods in Natural Language Processing, EMNLP 2015, Lisbon, Portugal, September 17-21, 2015*. The Association for Computational Linguistics, 1412–1421. <https://doi.org/10.18653/V1/D15-1166>
- [26] Teng Niu, Shuai Zhu, Lei Pang, and Abdulmoteleb El-Saddik. 2016. Sentiment Analysis on Multi-View Social Data. In *MultiMedia Modeling - 22nd International Conference, MMM 2016, Miami, FL, USA, January 4-6, 2016, Proceedings, Part II (Lecture Notes in Computer Science, Vol. 9517)*. Springer, 15–27. https://doi.org/10.1007/978-3-319-27674-8_2
- [27] Hongliang Pan, Zheng Lin, Peng Fu, Yatao Qi, and Weiping Wang. 2020. Modeling Intra and Inter-modality Incongruity for Multi-Modal Sarcasm Detection. In *Findings of the Association for Computational Linguistics: EMNLP 2020, Online Event, 16-20 November 2020 (Findings of ACL, Vol. EMNLP 2020)*. Association for Computational Linguistics, 1383–1392. <https://doi.org/10.18653/V1/2020.FINDINGS-EMNLP.124>
- [28] Juan Manuel Pérez, Juan Carlos Giudici, and Franco M. Luque. 2021. Pysentimiento: A Python Toolkit for Sentiment Analysis and SocialNLP tasks. *CoRR* abs/2106.09462 (2021). arXiv:2106.09462 <https://arxiv.org/abs/2106.09462>
- [29] Alec Radford, Jong Wook Kim, Chris Hallacy, Aditya Ramesh, Gabriel Goh, Sandhini Agarwal, Girish Sastry, Amanda Askell, Pamela Mishkin, Jack Clark, Gretchen Krueger, and Ilya Sutskever. 2021. Learning Transferable Visual Models From Natural Language Supervision. In *Proceedings of the 38th International Conference on Machine Learning, ICML 2021, 18-24 July 2021, Virtual Event (Proceedings of Machine Learning Research, Vol. 139)*. PMLR, 8748–8763. <http://proceedings.mlr.press/v139/radford21a.html>
- [30] Kihyuk Sohn. 2016. Improved Deep Metric Learning with Multi-Class N-pair Loss Objective. In *Advances in Neural Information Processing Systems 29: Annual Conference on Neural Information Processing Systems 2016, December 5-10, 2016, Barcelona, Spain*. 1849–1857. <https://proceedings.neurips.cc/paper/2016/hash/6b180037abbebae91d8b1232f8a8ca9-Abstract.html>

- [31] Aäron van den Oord, Yazhe Li, and Oriol Vinyals. 2018. Representation Learning with Contrastive Predictive Coding. arXiv:1807.03748 <http://arxiv.org/abs/1807.03748>
- [32] Ashish Vaswani, Noam Shazeer, Niki Parmar, Jakob Uszkoreit, Llion Jones, Aidan N. Gomez, Lukasz Kaiser, and Illia Polosukhin. 2017. Attention is All You Need. In *Advances in Neural Information Processing Systems 30: Annual Conference on Neural Information Processing Systems 2017, December 4-9, 2017, Long Beach, CA, USA*. 5998–6008. <https://proceedings.neurips.cc/paper/2017/hash/3f5ee243547dee91fbd053c1c4a845aa-Abstract.html>
- [33] Nan Xu, Wenji Mao, and Guandan Chen. 2019. Multi-Interactive Memory Network for Aspect Based Multimodal Sentiment Analysis. In *The Thirty-Third AAAI Conference on Artificial Intelligence, AAAI 2019, The Thirty-First Innovative Applications of Artificial Intelligence Conference, IAAI 2019, The Ninth AAAI Symposium on Educational Advances in Artificial Intelligence, EAAI 2019, Honolulu, Hawaii, USA, January 27 - February 1, 2019*. AAAI Press, 371–378. <https://doi.org/10.1609/AAAI.V33I01.3301371>
- [34] Hsueh-Cheng Wang and Marc Pomplun. 2011. The Attraction of Visual Attention to Texts in Real-World Scenes. In *Proceedings of the 33th Annual Meeting of the Cognitive Science Society, CogSci 2011, Boston, Massachusetts, USA, July 20-23, 2011*. cognitivesciencesociety.org. <https://mindmodeling.org/cogsci2011/papers/0630/index.html>
- [35] Yiwei Wei, Shaozu Yuan, Ruosong Yang, Lei Shen, Zhangmeizhi Li, Longbiao Wang, and Meng Chen. 2023. Tackling Modality Heterogeneity with Multi-View Calibration Network for Multimodal Sentiment Detection. In *Proceedings of the 61st Annual Meeting of the Association for Computational Linguistics (Volume 1: Long Papers), ACL 2023, Toronto, Canada, July 9-14, 2023*. Association for Computational Linguistics, 5240–5252. <https://doi.org/10.18653/V1/2023.ACL-LONG.287>
- [36] Changsong Wen, Guoli Jia, and Jufeng Yang. 2023. DIP: Dual Incongruity Perceiving Network for Sarcasm Detection. In *IEEE/CVF Conference on Computer Vision and Pattern Recognition, CVPR 2023, Vancouver, BC, Canada, June 17-24, 2023*. Computer Vision Foundation / IEEE, 2540–2550. <https://doi.org/10.1109/CVPR52729.2023.00250>
- [37] Xuehua Wu, Jin Mao, Hao Xie, and Gang Li. 2022. Identifying humanitarian information for emergency response by modeling the correlation and independence between text and images. *Information Processing & Management* 59, 4 (2022), 102977. <https://doi.org/10.1016/J.IPM.2022.102977>
- [38] Nan Xu. 2017. Analyzing Multimodal Public Sentiment Based on Hierarchical Semantic Attentional Network. In *IEEE International Conference on Intelligence and Security Informatics, ISI 2017, Beijing, China, July 22-24, 2017*. IEEE, 152–154. <https://doi.org/10.1109/ISI.2017.8004895>
- [39] Nan Xu and Wenji Mao. 2017. MultiSentiNet: A Deep Semantic Network for Multimodal Sentiment Analysis. In *Proceedings of the 2017 ACM on Conference on Information and Knowledge Management, CIKM 2017, Singapore, November 06 - 10, 2017*. ACM, 2399–2402. <https://doi.org/10.1145/3132847.3133142>
- [40] Nan Xu, Wenji Mao, and Guandan Chen. 2018. A Co-Memory Network for Multimodal Sentiment Analysis. In *The 41st International ACM SIGIR Conference on Research & Development in Information Retrieval, SIGIR 2018, Ann Arbor, MI, USA, July 08-12, 2018*. ACM, 929–932. <https://doi.org/10.1145/3209978.3210093>
- [41] Xiaocui Yang, Shi Feng, Daling Wang, and Yifei Zhang. 2021. Image-Text Multimodal Emotion Classification via Multi-View Attentional Network. *IEEE Transactions on Multimedia* 23 (2021), 4014–4026. <https://doi.org/10.1109/TMM.2020.3035277>
- [42] Xiaocui Yang, Shi Feng, Yifei Zhang, and Daling Wang. 2021. Multimodal Sentiment Detection Based on Multi-channel Graph Neural Networks. In *Proceedings of the 59th Annual Meeting of the Association for Computational Linguistics and the 11th International Joint Conference on Natural Language Processing, ACL/IJCNLP 2021, (Volume 1: Long Papers), Virtual Event, August 1-6, 2021*. Association for Computational Linguistics, 328–339. <https://doi.org/10.18653/V1/2021.ACL-LONG.28>
- [43] Jianfei Yu and Jing Jiang. 2019. Adapting BERT for Target-Oriented Multimodal Sentiment Classification. In *Proceedings of the Twenty-Eighth International Joint Conference on Artificial Intelligence, IJCAI 2019, Macao, China, August 10-16, 2019*. ijcai.org, 5408–5414. <https://doi.org/10.24963/IJCAI.2019/751>
- [44] Lin Yue, Weitong Chen, Xue Li, Wanli Zuo, and Minghao Yin. 2019. A Survey of Sentiment Analysis in Social Media. *Knowledge and Information Systems* 60, 2 (2019), 617–663. <https://doi.org/10.1007/S10115-018-1236-4>
- [45] Lei Zhang, Shuai Wang, and Bing Liu. 2018. Deep Learning for Sentiment Analysis: A Survey. *Wiley Interdisciplinary Reviews: Data Mining and Knowledge Discovery* 8, 4 (2018). <https://doi.org/10.1002/WIDM.1253>
- [46] Yi Zhang, Mingyuan Chen, Jundong Shen, and Chongjun Wang. 2022. Tailor Versatile Multi-Modal Learning for Multi-Label Emotion Recognition. In *The Thirty-Sixth AAAI Conference on Artificial Intelligence, AAAI 2022, Thirty-Fourth Conference on Innovative Applications of Artificial Intelligence, IAAI 2022, The Twelfth Symposium on Educational Advances in Artificial Intelligence, EAAI 2022 Virtual Event, February 22 - March 1, 2022*. AAAI Press, 9100–9108. <https://doi.org/10.1609/AAAI.V36I8.20895>
- [47] Sicheng Zhao, Xingxu Yao, Jufeng Yang, Guoli Jia, Guiguang Ding, Tat-Seng Chua, Björn W. Schuller, and Kurt Keutzer. 2022. Affective Image Content Analysis: Two Decades Review and New Perspectives. *IEEE Transaction on Pattern Analysis and Machine Intelligence* 44, 10 (2022), 6729–6751. <https://doi.org/10.1109/TPAMI.2021.3094362>
- [48] Peng Zhou, Wei Shi, Jun Tian, Zhenyu Qi, Bingchen Li, Hongwei Hao, and Bo Xu. 2016. Attention-Based Bidirectional Long Short-Term Memory Networks for Relation Classification. In *Proceedings of the 54th Annual Meeting of the Association for Computational Linguistics, ACL 2016, August 7-12, 2016, Berlin, Germany, Volume 2: Short Papers*. The Association for Computer Linguistics. <https://doi.org/10.18653/V1/P16-2034>